

# Human Modeling for Autonomous Vehicles: Reachability Analysis, Online Learning, and Driver Monitoring for Behavior Prediction

*Vijay Govindarajan  
Ruzena Bajcsy*

Electrical Engineering and Computer Sciences  
University of California at Berkeley

Technical Report No. UCB/EECS-2017-226

<http://www2.eecs.berkeley.edu/Pubs/TechRpts/2017/EECS-2017-226.html>

December 15, 2017



Copyright © 2017, by the author(s).  
All rights reserved.

Permission to make digital or hard copies of all or part of this work for personal or classroom use is granted without fee provided that copies are not made or distributed for profit or commercial advantage and that copies bear this notice and the full citation on the first page. To copy otherwise, to republish, to post on servers or to redistribute to lists, requires prior specific permission.

### Acknowledgement

I would like to thank my advisor, Ruzena Bajcsy, for providing the amazing learning opportunity of working in her lab and for her support. I have gained a deeper appreciation for the challenges of human modeling and designing effective experiments.

I would also like to thank Katie Driggs-Campbell for her extensive guidance and encouragement. The chapters in the thesis were based on joint work I did with Katie. I have learned a great deal from her experience in driver modeling and experiment design.

Gregorij Kurillo helped with the camera calibration setup. Robert Matthew and Joseph Gavazza provided support for the thermal camera mount.

Funding was provided by ONR MURI N000141310341, DURIP

N000141310679, NSF 1545126, Aisin Technical Center of America, and Berkeley DeepDrive.

**Human Modeling for Autonomous Vehicles: Reachability Analysis, Online Learning, and Driver Monitoring for Behavior Prediction**

by

Vijay Govindarajan

A thesis submitted in partial satisfaction of the

requirements for the degree of

Master of Science

in

Electrical Engineering and Computer Sciences

in the

Graduate Division

of the

University of California, Berkeley

Committee in charge:

Professor Ruzena Bajcsy, Chair

Professor Trevor Darrell

Fall 2017



---

**Human Modeling for Autonomous Vehicles: Reachability Analysis,  
Online Learning, and Driver Monitoring for Behavior Prediction**

by Vijay Govindarajan

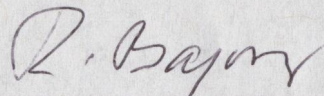
---

**Research Project**

Submitted to the Department of Electrical Engineering and Computer Sciences,  
University of California at Berkeley, in partial satisfaction of the requirements for the  
degree of **Master of Science, Plan II.**

Approval for the Report and Comprehensive Examination:

**Committee:**



---

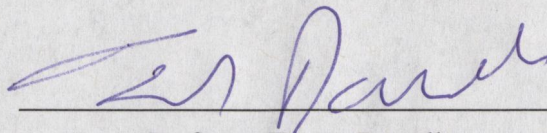
Professor Ruzena Bajcsy  
Research Advisor

12/06/2017

---

(Date)

\*\*\*\*\*



---

Professor Trevor Darrell  
Second Reader

12/07/2017

---

(Date)

## Abstract

Human Modeling for Autonomous Vehicles: Reachability Analysis, Online Learning, and Driver Monitoring for Behavior Prediction

by

Vijay Govindarajan

Master of Science in Electrical Engineering and Computer Sciences

University of California, Berkeley

Professor Ruzena Bajcsy, Chair

In order to design safe and effective human-in-the-loop systems, developing robust and useful models of human behavior is absolutely vital. However, this problem is highly difficult to address, given that humans often act unpredictably. We look at two approaches to model the human agent: one motivated by safety and capturing the likely behaviors across a wide range of human agents, and another motivated by personalization and adapting control to the specific human user.

In the first approach, we investigate the problem of determining prediction sets for human-driven vehicles using Hamilton-Jacobi reachability analysis and empirical observations from driving datasets. Given evaluation metrics of accuracy, precision, and risk, we optimize disturbance bounds to construct forward reachable sets with high precision that satisfy accuracy and risk constraints. To demonstrate the approach, we apply our framework to a lane changing scenario to provide set predictions that provide safety guarantees without being over-conservative. We show an example of this method that allows us to construct a reachable set with over 85% accuracy and under 25% risk.

In the second modeling approach, we seek to model the human as a collaborator and use the state of the driver to develop an adaptive assistance system. We focus on the problem of measuring the driver state under varying levels of cognitive workload using affective (i.e. emotion) sensing, including facial analysis and electroencephalography (EEG). This information is then used to help predict the brake reaction time of the driver, a key input in designing forward collision warning systems. We use online learning methods, as a way for the autonomous system to gradually learn from examples and improve predictions over time. We then demonstrate the results in a pilot study, which shows that while detecting the cognitive task is challenging, affective sensing can be used directly to reduce prediction error or speed up learning of brake reaction time for some individuals. We then end with some improvements that can be made to further strengthen the quality of the affective sensing-based prediction models in future work.

# Contents

<b>Contents</b>	<b>i</b>
<b>1 Introduction</b>	<b>1</b>
<b>2 Data-Driven Reachability Analysis for Human-in-the-Loop Systems</b>	<b>2</b>
2.1 Introduction . . . . .	2
2.2 Related Works . . . . .	3
2.3 Methodology . . . . .	5
2.4 Implementation . . . . .	8
2.5 Evaluation and Results . . . . .	10
2.6 Discussion and Future Work . . . . .	12
<b>3 Driver State Monitoring and Online Learning for Personalized Driver Assistance Systems</b>	<b>13</b>
3.1 Introduction . . . . .	13
3.2 Literature Review . . . . .	14
3.3 Experimental Design . . . . .	17
3.4 Methodology . . . . .	22
3.5 Results . . . . .	25
3.6 Discussion . . . . .	26
<b>Bibliography</b>	<b>29</b>

# Chapter 1

## Introduction

A key challenge in human-robot interaction is developing high fidelity models for the human agent. Without these models, the robot agent cannot properly predict human behaviors and respond appropriately. This problem is difficult, however, given the unpredictability of the human agent. Thus, there is a tradeoff between trying to be robust to all possible sets of human behavior, or focusing solely on the most likely actions. Another challenge is that each human is different. Each person has varying physical and cognitive capabilities and different preferences and expectations from the robot agent. In addition, they may change preferences over time, based on their affective (emotional) state. This problem is especially relevant in the intelligent vehicle domain, where autonomous vehicles must collaborate with human passengers and other human drivers.

This thesis consists of two approaches to modeling the human agent in the intelligent vehicle setting. Chapter 2 discusses how an empirical approach using large scale driving datasets can be used with reachability analysis to provide prediction sets on human behavior that balance accuracy, risk, and precision constraints. This approach is suitable for modeling a wide variety of human agents. In contrast, Chapter 3 focuses on personalization of driver assistance systems using online learning and affective (emotion) state monitoring to develop a tailored human behavior model. This approach can be used to design systems that not only take into account the specific human user but also adapt control behavior as a function of the affective state.



## Chapter 2

# Data-Driven Reachability Analysis for Human-in-the-Loop Systems

### 2.1 Introduction

A crucial problem in human-robot interaction and human-in-the-loop control is designing control algorithms that are both safe and effective [11]. In order to design such control frameworks, rigorous models of human behaviors and dynamics are required. This, however, is rather challenging, as humans are unpredictable and describing their behavior via standard dynamical methods is often difficult [46].

Intelligent vehicles are a key application of human-in-the-loop control, as human drivers directly influence the system on many different levels. From one perspective, drivers interact directly with active safety systems that intervene and assist the driver to maintain safe behaviors [7]. From the autonomous perspective, human drivers will be influencing and cooperating with autonomous vehicles on the road, meaning their anticipated actions must be integrated into autonomous vehicle control [10].

While autonomous vehicle technology has advanced rapidly, there still remain obstacles to full integration on current roadways. Eventually, communication protocols like V2V or V2I will facilitate this process [45]. However, in the short term, autonomous vehicles will have to operate in mixed environments, with both human-driven and autonomous vehicles on the road. The challenge is how to seamlessly introduce autonomy into such environments [9].

This work presents a method for modeling the likely behaviors of humans as reachable sets that are chosen based on empirical observations from driving datasets. The motivating example for this work is shown in Figure 2.1. This example reveals an inherent trade-off. We can be conservative and capture all likely behaviors, or we can try to make a more informative prediction by only capturing the most likely behaviors. In this work, we investigate this trade-off by constructing and evaluating forward reachable sets for vehicles based on Hamilton-Jacobi reachability analysis and observations from a driving dataset. In

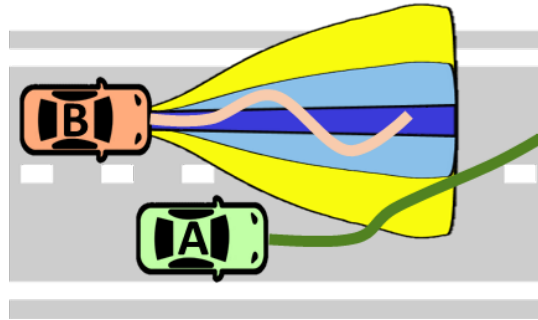


Figure 2.1: We wish to find the correct reachable set to model the behaviors of vehicle B. Here, the yellow set is over-conservative with respect to vehicle A’s trajectory (green). In contrast, the dark blue set does not fully capture the behavior of vehicle B, as evidenced by vehicle’s B actual trajectory (light orange) leaving the set. Thus, the light blue set is the best balance.

addition, we investigate how to maximize precision of the reachable set given accuracy and risk constraints.

This chapter is organized as follows. The following section highlights related studies in human modeling and human-in-the-loop control. Section 2.3 describes the problem formulation, evaluation metrics, and optimization approach. The methods used to compute the reachable sets are detailed in Section 2.4. Section 2.5 presents the evaluation metrics for the computed reachable sets and provides an example implementation of the aforementioned optimization problem. Finally, Section 2.6 includes discussion and future work.

## 2.2 Related Works

In order to have safe and interactive systems, predictive modeling is incredibly important [10]. There is a rich body of literature on human prediction and human-in-the-loop control. We aim to find a balance between *informativeness* and *conservativeness* as it applies to predictive modeling.

Ideally, for each obstacle in the environment, the exact future trajectory would be known. This precise trajectory would be maximally *informative*. However, given the randomness of human motion, it is unlikely that the precise trajectory will be uncovered uniquely [46]. In the realm of intelligent vehicles, many works have developed models that attempt to predict the exact trajectory, but either do not generalize well or cover unknown situations [19]. Stochastic models have also been developed, but make many assumptions on the underlying model of human behavior (e.g. Markov Decision Processes assume humans satisfy the Markov property [1]) or on the distribution on human actions [9].

In contrast to informative models, reachable sets maximize the *conservativeness* of the prediction by capturing worst-case behavior under specified disturbance bounds. Reachability analysis is a well developed tool that provides guarantees on safe behaviors for control systems [47]. This methodology has been effectively used in many settings for provably

correct control, optimal control for hybrid systems, and multi-agent applications.

Further, these and related methods can provide certificates that give an exact proof of safety [39]. By using such approaches, which rely on dynamical models, many issues with discretization and the common “signal to symbol” problem are mitigated [44]. In order to utilize these techniques, many assumptions must be made on the model being used. For instance, typically the dynamics and model parameters must be known (and relatively simple to address complexity issues) and the disturbance bounds must be predetermined [31]. There has been a great deal of work aiming to address these issues by considering stochastic reachability or by applying safe learning techniques.

Many stochastic reachability approaches rely on discretization by modeling the system as a Markov Decision Process [18]. This has been successfully applied to traffic scenarios to guarantee safe maneuvers on the road [3]. Similarly, stochastic reach-avoid formulations have shown promising results in multi-agent autonomous settings [22]. In [27], stochastic reachable sets were used in a path planning framework, assuming discrete modes of behavior for each obstacle. While this work is promising, the approach lacks the generality of the continuous domain and requires assumptions that might not hold for human-in-the-loop systems [9].

For human-controlled systems, disturbances are often difficult to model and use in control frameworks [43]. The selection of disturbance bounds, however, is crucial—if the assumed bounds do not globally capture the true disturbance, reachability analysis can no longer guarantee safety. On the other hand, if the disturbances are over-approximated, the resulting control will be over-conservative [10].

To address this, there has been growing interest in learning these disturbances online to reduce the conservativeness of these methods [13]. These concepts have been used in safe online learning frameworks that learn control policies via reinforcement learning while simultaneously learning disturbances and modeling errors [2].

In this work, we aim to relax the assumptions required to develop safe, interactive human-in-the-loop systems by using empirical methods in order to (1) learn disturbances and (2) balance informativeness and conservativeness. This approach allows us to capture the wide variety of human behaviors and express these observations succinctly using reachability analysis, which provides a certificate on safety.

We aim to empirically optimize the disturbance bounds used to generate useful forward reachable set predictions. When forward reachable sets are used to predict sets of possible trajectories, they provide nice safety guarantees, subject to some assumptions on disturbance input bounds that might not hold in practice. To address this, we evaluate the effectiveness of these sets for predicting human driven vehicles trajectories, identifying the correct disturbances for *conservative* and *informative* predictions.

In addition, supposing we have an accurate prediction that provide safety bounds for interaction, we assess how these are violated by other agents on the road. This gives us a measure of how *over-conservative* the prediction set is with respect to interaction. By applying empirical analysis to reachability analysis, we can generate useful set predictions while maintaining a certificate on safety.

## 2.3 Methodology

This section presents the formalization of how we aim to model the human and the interaction with other vehicles. We outline how the parameters of this model can be optimized to generate useful reachable set predictions, using empirical evaluation metrics as constraints.

### Problem Formulation

Suppose we have a human driven vehicle, which we will represent with a simplified kinematic model:

$$\begin{aligned} \dot{x} &= v \cos(\theta) \\ \dot{y} &= v \sin(\theta) \\ \dot{\theta} &= \omega \\ v &\in D_v \\ \omega &\in D_\omega \end{aligned} \tag{2.1}$$

where  $x$  and  $y$  denote the vehicle's position,  $\theta$  denotes the vehicle's heading,  $v$  denotes the vehicle's speed, and  $\omega$  is the vehicle's steering rate. As this is a human driven vehicle, we suppose that there is uncertainty in the control of the vehicle, denoted  $D_v$  and  $D_\omega$ , which are compact sets in  $\mathbb{R}$ . It is assumed that all other sources of noise and uncertainty are encompassed by these disturbance sets.

Further, we assume we are able to compute the forward reachable set for a fixed time horizon,  $T$ , which will be denoted  $\Delta(D_v, D_\omega)$  or  $\Delta$  for simplicity. Given that methods for computing this set are well-studied, we focus our attention on identifying the tunable parameters, i.e. the disturbances.

In order to properly assess and optimize this set, we assume the existence of a human-in-the-loop dataset of driving behaviors and interactions. We focus on scenarios similar to Figure 2.1, where vehicle A seeks to merge in front of vehicle B. The reachable set is used to model possible actions of vehicle B, and risk is measured by evaluating the level of intrusion by vehicle A into this set. Thus, we have a set of trajectories representing the in-lane vehicle  $X^B$  and the other vehicle  $X^A$ . Given our motivating example (Figure 2.1), we will denote an instance of a lane change execution and the corresponding reaction as a pair of trajectories, denoted  $x_t^A \in X^A$  and  $x_t^B \in X^B$ .

By relaxing strict bounds on safety and interaction, we are able to sacrifice conservativeness for informativeness. However, this is a difficult problem to solve in general, given that (1) computing the reachable set is difficult; (2) these constraints are not easily written as simple constraints; and (3) these constraints are at odds with one another. The following sections describe how we use empirical methods and an iterative optimization procedure to address this problem.

## Set Evaluation Metrics

We introduce three metrics to evaluate the results and provide empirical constraints for optimization.

- 1) *Accuracy Metric*: Does the actual trajectory lie within the prediction set?
- 2) *Precision Metric*: How informative is this predictive set when compared to a generic set prediction?
- 3) *Risk Metric*: How frequently is this set violated by the other agent?

In essence, we would like to verify that we are reliably predicting driver behavior, that we are using a set prediction that is relatively small and informative, and that the set is not over-conservative with respect to interaction.

We formalize these metrics in the following equations. Accuracy is defined as:

$$A = \frac{1}{L} \sum_{l=1}^L \mathbb{I}\{x_l^B \in \Delta\} \quad (2.2)$$

where  $L$  is the number of lane changes,  $\mathbb{I}$  is the indicator function,  $x_l^B$  is element  $l$  in a library of trajectories  $X^B$ , and  $\Delta$  is the reachable set generated to predict the possible behaviors of vehicle  $B$ .

This averages the instances in which the vehicle  $B$ 's trajectory was correctly predicted as falling within the set.

Precision is defined as:

$$P = 1 - \frac{\lambda(\Delta)}{\lambda(\Lambda)} \quad (2.3)$$

where  $\lambda(\cdot)$  is the Lebesgue measure that gives the size of the set,  $\Delta$  is the predicted set for vehicle  $B$ , and  $\Lambda$  represents a generic prediction set for the vehicle. In this case, the reachable set generated using the largest disturbance bounds investigated (refer to Table 2.1) was used as  $\Lambda$ .

Precision gives us an idea of how informative the set  $\Delta$  is by assessing how much we are shrinking the set from the set prediction using the largest confidence bounds.

If the precision metric is 1, the size of the prediction set is 0, meaning that we have precisely predicted the exact trajectory. If the precision metric is 0, then we are not reducing the size of the set and we can surmise that this prediction is not informative.

The reachable set formulation provides a set of states that the vehicle of interest (i.e. vehicle  $B$ ) may visit in a given time horizon. The boundaries of this set provide safety guidelines that can be used by adjacent vehicles (i.e. vehicle  $A$ ) on the road for planning, given that disturbance bound assumptions on vehicle  $B$  hold. However, humans often violate these safety boundaries. For example, in a high traffic situation, there simply may not be enough space to maintain a large lane gap and still make a lane change. To quantify how risky a human behaves with respect to a given reachable set, we develop interaction metrics that capture how much a given trajectory intrudes on the reachable set. Here, we focus on a *risk* metric,  $R$ , defined analogously to the accuracy metric:

$$R = \frac{1}{L} \sum_{l=1}^L \mathbb{I}\{x_l^A \cap \Delta \neq \emptyset\} \quad (2.4)$$

where  $x_l^A$  is the trajectory of the adjacent vehicle (A) that merges and  $\Delta$  is the set of predictions for vehicle in lane (B). We wish to see if the adjacent vehicle enters the reachable set for the vehicle in lane. The risk metric determines, for the given dataset, how often the adjacent vehicle intrudes on the reachable set.

If the risk metric is 0, then the set  $\Delta$  is never intruded on by vehicle A and can be treated as a hard safety bound for planning by vehicle A. In contrast, if the risk metric is 1, then that implies the set  $\Delta$  is over-conservative, as the adjacent vehicle never avoided this set.

## Set Optimization Problem

We would like to find the set that maximizes precision (i.e. informativeness) subject to constraints on accuracy (i.e. conservativeness) and risk. We formalize this as the following optimization problem:

$$\begin{aligned} & \underset{D_v \subset \mathbb{R}, D_\omega \subset \mathbb{R}}{\text{maximize}} && P(\Delta(D_v, D_\omega)) \\ & \text{subject to} && A(\Delta(D_v, D_\omega)) \geq \bar{a} \\ & && R(\Delta(D_v, D_\omega)) \leq \bar{r} \end{aligned} \tag{2.5}$$

where  $\Delta(D_v, D_\omega) \subset \mathbb{R}^n$  is the reachable set prediction generated using disturbance bounds  $D_v$  and  $D_\omega$ .  $P(\cdot)$ ,  $A(\cdot)$ , and  $R(\cdot)$ , are as defined in Section 2.3.

To make this problem well-posed, we optimize over one constraint at a time. We write this nested problem as follows:

$$\begin{aligned} (D_v^*, \omega_1^*) \leftarrow & \underset{D_v \subset \mathbb{R}, \omega_1 \in \mathbb{R}}{\text{argmax}} && P(\Delta(D_v, D_\omega)) \\ & \text{subject to} && A(\Delta(D_v, D_\omega)) \geq \bar{a} \\ & && D_\omega = [\omega_1, \omega_2^*] \\ \omega_2^* \leftarrow & \underset{\omega_2 \in \mathbb{R}}{\text{argmax}} && \lambda(D_\omega) \\ & \text{subject to} && R(\Delta(D_v^*, D_\omega)) \leq \bar{r} \\ & && D_\omega = [\omega_1^*, \omega_2] \end{aligned} \tag{2.6}$$

where the steering disturbance is separated into its bounds  $D_\omega = [\omega_1, \omega_2]$ , and size of the set is given by the Lebesgue measure  $\lambda(\cdot)$  and all other variables are as previously defined.

The separation of disturbance sets and constraints simplifies the optimization program and allows for the competing objectives to be optimized iteratively, depending on what metric is influenced (e.g. risk is mostly influenced by lateral motion in the direction of vehicle A).

This cost function is motivated by the fact that the reduction in the disturbance range will lead to a smaller reachable set, thus improving precision, as was proven in [2]. At the same time, the resulting reachable set will be large enough to capture the most likely behaviors at an acceptable level of risk. While the proposed optimization procedure would take too long for real-time implementation, solutions could be precomputed and stored in a look-up table for real-time planning and control.

## 2.4 Implementation

The following sections present the methods used for computing  $\Delta(D_v, D_\omega)$  via Hamilton-Jacobi reachability analysis and for calculating the optimal disturbance bounds.

### Reachable Sets

To capture the likely driving behaviors, we use forward reachable sets to determine the likely positions the vehicle may occupy in  $T=3$  seconds. This time horizon was chosen based on the following distance often used in practice [34].

The definition of forward reachable set used in this paper is the maximal forward reachable tube described in [29]. Specifically, we define the forward reachable set,  $\Delta$  as:

$$\Delta \triangleq \{x \in \mathcal{X} \mid \exists d \in \mathcal{D}, \exists x_0 \in \mathcal{X}_0, \exists t \in [0, T], s(t, 0, x_0, d) = x\} \quad (2.7)$$

where  $\mathcal{X}$  is the state space,  $\mathcal{D}$  is the space of possible disturbance input trajectories,  $\mathcal{X}_0$  is the set of initial states, and  $s(t, 0, x_0, d)$  is the state at time  $t \geq 0$  starting at initial state  $x_0$  subject to disturbance  $d$  that arises from the dynamics in Equation 2.1.

The forward reachable set is computed based on a Hamilton-Jacobi Partial Differential Equation (HJ PDE) formulation using the Level Set Toolbox [30]. In particular, the forward reachable set at time  $t$  is the zero sublevel set of  $J(x, t)$ , the solution to the following PDE:

$$\begin{aligned} \frac{\partial J}{\partial t} + \max_{v, \omega} \frac{\partial J}{\partial x} \cdot f(x, v, \omega) &= 0 \\ \text{subject to } J(x, 0) &= g(x) \\ v &\in D_v, \quad \omega \in D_\omega \end{aligned} \quad (2.8)$$

Here,  $g(x)$  is a implicit surface function for which the zero sublevel set is the initial condition set, and  $f(x, v, \omega)$  is the system evolution ODE in Equation 2.1.

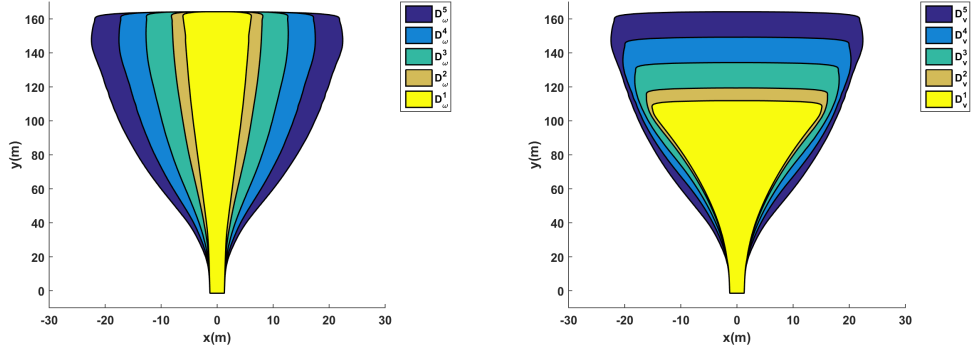
The Level Set Toolbox, which uses numerical methods to approximate the solution to Equation 2.8, requires an initial set and a grid resolution to be provided. For analysis, the initial set was an uncertainty region about the state  $(0, 0, \frac{\pi}{2})$ , i.e.  $x \in [-1.5, 1.5], y \in [-1.5, 1.5], \theta \in [\frac{\pi}{2} - 0.02, \frac{\pi}{2} + 0.02]$ . In addition, the grid for the solver was chosen to achieve roughly 0.5 m resolution in  $x$  and  $y$  and 0.005 rad resolution in  $\theta$ . The uncertainty in the initial set captures possible localization error and is large enough relative to the resolution for accurate numerical computation of the reachable set.

Sample reachable sets are shown in Figure 2.2 for varying disturbance bounds. The computed 3D (i.e.,  $x, y, \theta$ ) reachable sets are projected down to 2D (i.e.,  $x, y$ ) for analysis.

### Dataset for Empirical Validation

In order to compute the metrics and validate our approach, we require a dataset of interactions,  $X^A$  and  $X^B$ , as detailed in Section 2.3. To get these sample trajectories, we use the NGSIM dataset, which has been used to do microscopic traffic modeling [16]. From the full





(a) Reachable sets generated with  $D_v$  fixed at  $D_v^5$  and  $D_\omega$  varied from  $D_\omega^1$  to  $D_\omega^5$ . As the turning rate increases, so does lateral deviation.  
 (b) Reachable sets generated with  $D_\omega$  fixed at  $D_\omega^5$  and  $D_v$  varied from  $D_v^1$  to  $D_v^5$ . As speed increases, both lateral and longitudinal deviation increase.

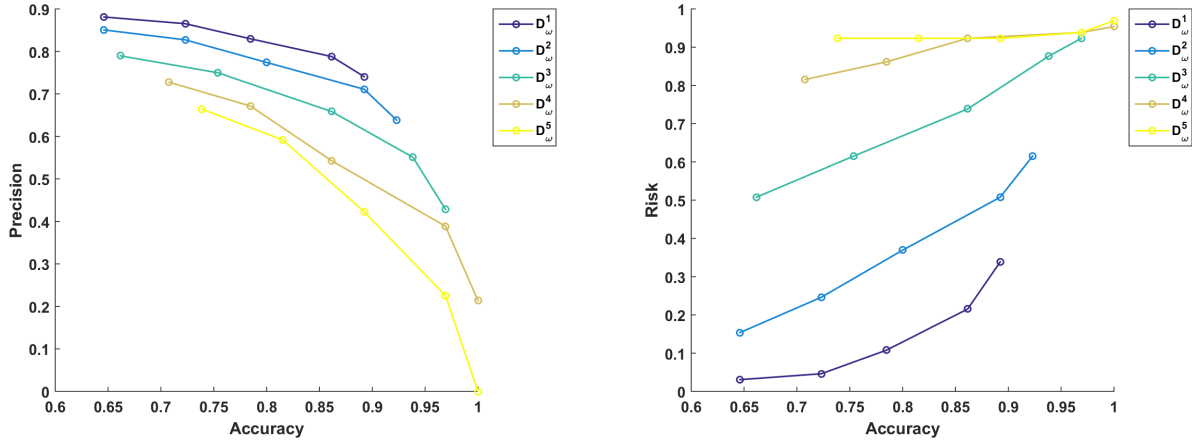
Figure 2.2: Sample forward reachable sets,  $T = 3s$ , based on varying  $D_v$  and  $D_\omega$  bounds detailed in Table 2.1.

dataset from the US Highway 101, we select lane change scenarios that match the scenario presented in Figure 2.1, resulting in 65 samples.

Using this data, we can compute the precision, accuracy, and risk for various disturbance bounds. The predetermined sets were chosen using disturbance bounds consistent with the empirical distributions in the data. The resulting bounds that were selected are shown in Table 2.1. These bounds reflect the fact that, in the dataset, there was more variation in the longitudinal velocity than there was in turning rate.

Table 2.1: Disturbance bounds on  $D_v$  and  $D_\omega$  used to generate reachable sets.

	$\mathbf{v(m/s)}$		$\boldsymbol{\omega(rad/s)}$
$\mathbf{D}_v^1$	(32.5, 37.5)	$\mathbf{D}_\omega^1$	(-0.01, 0.01)
$\mathbf{D}_v^2$	(30.0, 40.0)	$\mathbf{D}_\omega^2$	(-0.02, 0.02)
$\mathbf{D}_v^3$	(25.0, 45.0)	$\mathbf{D}_\omega^3$	(-0.04, 0.04)
$\mathbf{D}_v^4$	(20.0, 50.0)	$\mathbf{D}_\omega^4$	(-0.06, 0.06)
$\mathbf{D}_v^5$	(15.0, 55.0)	$\mathbf{D}_\omega^5$	(-0.08, 0.08)



(a) Accuracy vs. Precision Trade-off Curves. (b) Accuracy vs. Risk Curves. For a fixed  $D_\omega$ -bound, we observe how accuracy and intrusion accuracy and precision change with the  $D_v$ -bound. change with the  $D_v$ -bound. As the set size becomes larger, risk increases. As precision increases, accuracy is sacrificed.

Figure 2.3: Set Evaluation Metric Curves.

## 2.5 Evaluation and Results

Given the reachable sets, we characterize conservativeness and informativeness via accuracy and precision metrics. We also determine the level of set violation based on the risk metric. Finally, we describe an example solution to the optimization problem detailed in Equation 2.6. These results are discussed in the following sections.

### Empirical Metrics

The trade-off between accuracy and precision is demonstrated in Figure 2.3a. The key result is that we can choose between high accuracy and high precision; achieving both objectives is not feasible. Figure 2.3b shows that as the size of the reachable set increases and accuracy goes up, so does the risk level with respect to that set.  $D_\omega^4$  and  $D_\omega^5$  have similar accuracy vs. risk profiles with high risk, suggesting that  $D_\omega^5$  may be over-conservative.

It is important to note that these are a sample of reachable sets based on preselected disturbance bounds. While this sample is adequate to illustrate the relationships between accuracy and precision and between accuracy and risk, it does not demonstrate how to actually construct a set that solves the optimization problem detailed in Equation 2.6. We next discuss how to get a suitably precise set to meet accuracy and risk requirements.

## Prediction Set Optimization with Empirical Constraints

So far, we have constructed reachable sets based on disturbance bounds that offer varying levels of accuracy and precision. We then saw that humans violate these safety sets in practice. The question then becomes how to choose the right set given these relationships. Given a risk profile of a given driver in vehicle A, we wish to pick the reachable set for vehicle B that has high precision but also satisfies constraints on accuracy and risk.

To solve this problem, we look at the optimization framework outlined in Equation 2.6. The key changes are that we start with a collection of precomputed reachable sets based on bounds in Table 2.1, for simplicity. We use a greedy approach to solve the problem.

For analysis, we choose disturbances such that  $D_\omega = [\omega_1, \omega_2]$ , where  $\omega_i \in \mathcal{W}_i, i = 1, 2$ . The sets are partitioned into positive and negative turning rates, i.e.  $\mathcal{W}_1 = \{-0.01, -0.02, -0.04, -0.06, -0.08\}$  and  $\mathcal{W}_2 = \{0.01, 0.02, 0.04, 0.06, 0.08\}$ . For this choice of  $\mathcal{W}_1$ , it was noted that  $\omega_1$  did not impact risk, as the dataset involved lane changes from the right. Thus,  $D_v$  and  $\omega_1$  were chosen to optimize precision subject to the accuracy constraint in the first step. In the second step,  $\omega_2$  was maximized subject to a risk constraint. The final result is a precise set that is sufficiently accurate but not too risky.

Figure 2.4 shows an example of how the set is morphed to achieve constraints on accuracy and risk level.

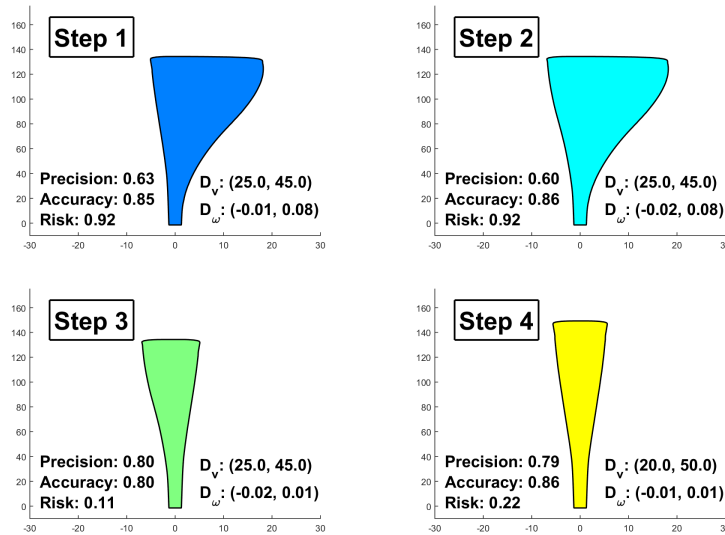


Figure 2.4: Sample set optimization with  $\bar{r} = 0.25$  and  $\bar{a} = 0.85$ . (1) The initial set is chosen at random. The accuracy (0.846) is just under the constraint. (2)  $D_v$  and  $\omega_1$  are optimized subject to accuracy while holding  $\omega_2$  constant. To achieve the accuracy constraint, the set is enlarged. (3) Next,  $\omega_2$  is optimized subject to risk holding the other two variables constant, shrinking the set. (4) The final set is chosen by increasing the bound on  $D_v$  but shrinking  $\omega_1$ . No further improvement in risk is possible in the next step, so the algorithm converges.

## 2.6 Discussion and Future Work

We looked at the problem of constructing reachable sets for a given vehicle based on accuracy and risk constraints. The disturbances used to generate these sets were informed by empirical observations from a driving dataset. The trade-off between conservative, accurate sets and informative, useful sets was also investigated. An advantage of the present approach is interpretability: given bounded disturbance inputs, we have safety guarantees based on the resulting reachable set. However, we have little idea of how likely the vehicle is to occupy a given subset of the state space. Thus stochastic reachable sets would be an interesting point of comparison for future work.

In addition, there is room to tie in the optimization problem more directly into the reachable set computation. Rather than precomputing a collection of sets, one can use the optimization framework to iteratively tune the disturbance parameters and recompute the reachable set with these updated values. Additionally, one can look at examining the state of the driver (e.g. drowsy, distracted) and tying in this information to tune levels of risk and accuracy. Incorporating sensing into the set prediction procedure will enable more adaptable human-in-the-loop systems.

## Chapter 3

# Driver State Monitoring and Online Learning for Personalized Driver Assistance Systems

### 3.1 Introduction

In the previous chapter, we developed a prediction model for the human agent that traded off some accuracy and accepted some risk in the hope of achieving higher precision and more useful sets from an human-robot collaboration perspective. This approach has benefits: it provides a certificate on safety subject to accuracy and risk levels, allowing us to design human-robot control algorithms for a wide variety of human users and collaborators.

However, this method does not include personalization. The algorithms are not tuned to the human actually using the autonomous system, which can result in suboptimal performance for a specific human user. As an example, if a collision warning system provides alerts too early or too late, then the driver may find the system either annoying or not trustworthy. Consequently, he or she may not use the system, eliminating any potential safety benefits of the alert system. To address this limitation, we decided to explore the problem of personalization for advanced driver assistance systems (ADAS). The motivation was to use the state of the driver, as captured through a variety of physiological sensors, to devise an adaptive control framework tailored for that individual.

There is current work in industry involving the application of AI and improved driver monitoring for personalized ADAS. Honda's Automated Network Assistant (HANA) is a project to analyze and respond to the driver's behavior. For example, HANA will adjust control performance as a function of the driver's level, acting more conservatively for beginners and allowing more flexibility for advanced drivers. In addition, HANA will include an "emotion engine" that measures parameters like the driver's facial expressions, voice, and heart rate to detect anxiety and stress and adapt its response accordingly [15]. Similarly, the Jaguar Land Rover "Sixth Sense" project aims to monitor the driver's heart rate, respi-

ration rate, and brain activity to detect stress and alertness. It will include haptic feedback through the steering wheel and/or pedals to help the driver refocus when the attention level is low [33].

There has also been work on developing personalized driver assistance systems. [5] use tunable control parameters to construct a lane change module that takes into account the driver's preference for longitudinal adjustment and gap acceptance. Similarly, [24] developed a human behavior prediction model to provide acceleration reference inputs to a MPC controller, resulting in human-like velocity control.

Given this interest, as well as the potential improvements in trust and safety with personalized systems, developing effective and tailored assistance systems is an important problem to address.

We focus on the problem of measuring the driver state under varying levels of cognitive workload using affective (i.e. emotion) sensing, including facial analysis and electroencephalography (EEG). This information is then used to help predict the brake reaction time of the driver, a key input in designing forward collision warning systems. We use online learning methods, as a way for the autonomous system to gradually learn from examples and improve predictions over time.

This chapter is organized as follows. The following section provides a literature review of online learning, affective sensing in driving, and forward collision warning alert systems. Section 3.3 outlines the experimental design, detailing the driving scenarios and how cognitive workload is varied. Section 3.4 discusses feature generation and the algorithms investigated for reaction time regression and cognitive task classification. Section 3.5 details the results for the regression and classification algorithms. Finally, Section 3.6 ends with a discussion of limitations and opportunities for future work.

## 3.2 Literature Review

### Motivation for Online Learning

To develop effective personalized models of human behavior, it helps to understand how humans learn and approach tasks and mimic these learning mechanisms.

In the human cognition literature, there has been a distinction made between procedural and episodic memory. The idea is that procedural memory refers to skills that are developed slowly with practice. In contrast, episodic memory corresponds to memory of past instances that is learned quickly. Reinforcement learning has been used to model procedural memory, while instance-based learning approaches have been used to model episodic memory. There may be a shift from episodic memory to procedural memory, as enough experience is gained over time [6].

Gonzelez et. al have proposed that the instance-based learning approach is the key learning mechanism in dynamic decision making. The idea is that when humans are faced with interdependent, time-constrained, and real-time decisions that have consequences on

the environment, they shift from a heuristic approach to past experience to make decisions. This led to the development of a cognitive architecture with instance-based learning theory used to explain human behavior[14].

With respect to human-robot interaction, instance-based learning approaches have been successfully used to transfer task knowledge from a human agent to a robot companion [37].

In this work, we focus on the case where the human provides examples incrementally, and the amount of examples collected is relatively low, making reinforcement learning approaches less effective. Thus, the online, instance-based learning approach is used to model human behavior.

## Affective Sensing

A key part of human cognition is their affective (i.e. emotional) state. [26] argued that the affective state can impact driving performance and developed a system to identify the driver's affective state using sensing like galvanic skin response, heart rate, and skin temperature.

While there is a large body of work on trying to predict the emotion from a variety of physiological sensors, we focus our attention on electroencephalography (EEG) and thermal facial analysis in this work. There are several related papers on sensing with EEG and thermal analysis. We highlight a couple of representative papers here.

EEG has been used to monitor attention levels and drowsiness. Most studies apply the Fast Fourier Transform to capture the frequency power-spectrum, which are then quantized into bands (e.g. alpha, beta, etc.). These powers are then used as features for classification or regression. [4] constructed a classifier to detect if the user was performing a psychomotor vigilance task (i.e. attentive) or relaxed with eyes open (i.e. not attentive). In addition, [25] looked at the problem of detecting driver drowsiness from EEG measurements, using the driver lane deviation as a proxy for drowsiness level.

Thermal imaging is a promising non-contact method to characterize the behavior of the autonomic nervous system (ANS). It has been used to measure perspiration, temperature variation in the skin, blood flow, cardiac pulse, and respiration patterns [20]. Thermal imaging can provide non-intrusive measurement of emotional behaviors that are difficult to spoof [38]. This approach has been used in a variety of applications, ranging from remote health monitoring to detect heart rate irregularities and sleep apnea [38] to stress detection [40].

## Forward Collision Warning Alert Systems

The application domain we are interested in personalizing is forward collision warning (FCW) alert systems. The timing of the alert is critical to the driver's acceptance of the FCW alert system, so tuning the timing for a specific driver may help boost acceptance and usefulness of the system.



Standard FCW approaches use either the time-to-collision (TTC) or a distance threshold to determine when an alert should be given. [8] provides an example of a vision-based FCW system using a fixed TTC threshold of 2 seconds.

In contrast to the standard FCW approach, [21] suggests that an adaptive FCW system may be preferable. With the standard approach, the alert is not tuned to a specific driver. If the alert is mistimed, the driver may lose confidence in the system. Consequently, the driver may not stop as quickly as expected or may turn off the alert for being too irritating. So any benefits of the FCW system would then be reduced. To solve this problem, the adaptive FCW approach uses the driver reaction time to tune the distance threshold used in the Stop Distance Algorithm (SDA) for collision warnings. A limitation of the adaptive FCW system used is the assumption that the reaction time is fixed for a given driver.

Our goal is to extend the adaptive FCW method by developing an online, adaptive FCW system that takes into account the driver affective state and improves over time with more data.

### 3.3 Experimental Design

This section provides an overview of the experiments run to assess the impact of cognitive workload on driver reaction time. Subjects were asked to drive in a simple braking scenario, where secondary cognitive tasks were added to increase workload. The goal of these experiments was to vary the workload level, measure the impact on the state of the driver with affective sensing, and use these measurements to help predict the driver's reaction time.

#### Driving Scenarios

The braking scenarios were developed using PreScan simulation software <sup>1</sup>, which enables development and testing of driver assistance systems. A Force Dynamics 401cr driving simulator was used to simulate forces experienced due to lateral (i.e. steering) or longitudinal (i.e. braking) acceleration <sup>2</sup>.

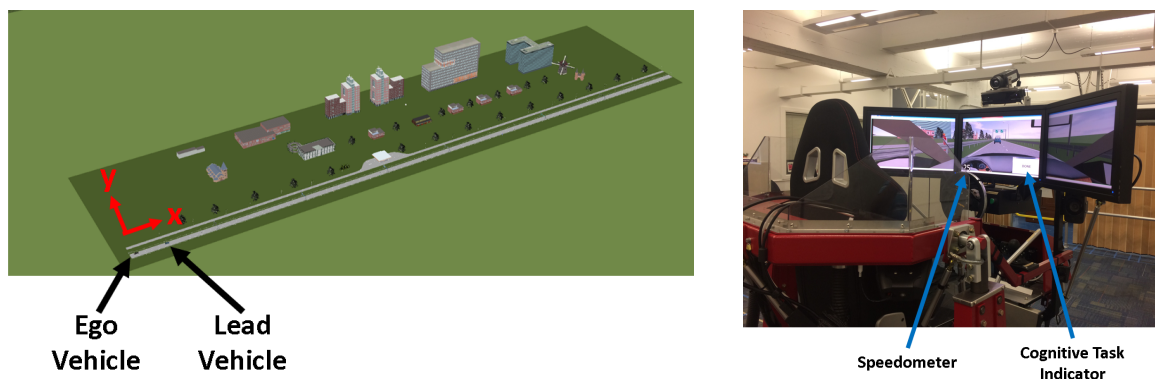
The driving environment consisted of two vehicles, a lead and ego vehicle. The lead vehicle's behavior was programmed, as detailed in Section 3.3. The ego vehicle was driven by the subject. An aerial view of the environment, along with the driver view, is provided in Figure 3.1.

#### Procedure

Six subjects were recruited for the driving study, including three males and three females. The age range varied from 23 to 36, and driving experience varied from less than 1 year to over 10 years.

<sup>1</sup><https://tass.plm.automation.siemens.com/prescan>

<sup>2</sup><https://www.force-dynamics.com/401>



(a) Aerial View of Driving Environment.

(b) Driver view of Driving Environment.

Figure 3.1: Driving Environment developed in PreScan. The subject drives the ego vehicle and follows a programmed lead vehicle. The driver's view also includes a speedometer and a task indicator to indicate the secondary cognitive task being evaluated.

Each subject was instructed to fill out surveys that assessed their driving experience. Then, a practice experiment trial was run to familiarize the subject with the driving simulator and the cognitive tasks. The subjects were given the following instructions:

- Try to maintain a constant speed (55 mph) if possible and stay in your lane with driving safely being your priority.
- At the start of each scenario, please release the steering wheel and place your foot over the accelerator.
- You may be given a secondary task to complete while driving. Please prioritize the driving task, but try to finish the secondary task as efficiently as you safely can.
- We'll be testing a series of different scenarios, which will occur in quick succession, meaning that after you have driven for about 25 seconds, a new scenario will automatically start under new conditions.

Ten trials, as detailed in Section 3.3, were conducted, with a short break (5-10 min) after every few trials. Each trial took roughly 8 minutes to complete.

At the end of the experiment, subjects filled out a post-experiment survey and the NASA TLX survey [17] to provide a self-reported measure of workload for the secondary cognitive tasks.

## Factors

Each trial consisted of four secondary tasks and four lead vehicle velocities, resulting in sixteen scenarios per trial. Ten trials were conducted for each subject. The two factors investigated are explained further below.

### Cognitive Workload Secondary Task

The primary factor varied was the cognitive workload secondary task. The focus on driver cognitive workload stems from the fact that the effect of cognitive workload on driver performance has been well-studied. The workload has been shown to impact both physiological measurements (e.g. heart rate, skin conductance, respiration rate) and driving performance [28].

The four secondary tasks given were:

1. No task
2. 0-back number recall task: subject simply repeats numbers as they are presented
3. 2-back number recall task: subject must say number two prior in the sequence as each new number is presented

4. Stroop visual task: subject must ignore word text and simply list the colors of each word in a table.

The  $n$ -back number tasks involve listening to a sequence of numbers played over a speaker, and then repeating the number  $n$  prior in the sequence. The n-back test was chosen due to its use in prior simulation and driving studies to adjust driver workload [28]. The N-backer implementation developed by Monk et al. was used to generate the number sequences and play the audio [32]. The same sequences were used for each subject, and each number was presented to the subject after a 2-second pause.

The Stroop task involves response inhibition and has been used for stress induction [41]. A set of color words (e.g. red, green, cyan, etc.) are presented in a window, but the color and text are incongruent. The task is to ignore the text of the given words and only say the colors of the words [42]. The Stroop task was conducted using a Matlab implementation developed by George Papazafeiropoulos<sup>3</sup>. The window was located on the same monitor as the driving visualization, so the subject could switch attention between the words and the driving scenario. An example is shown in Figure 3.2.



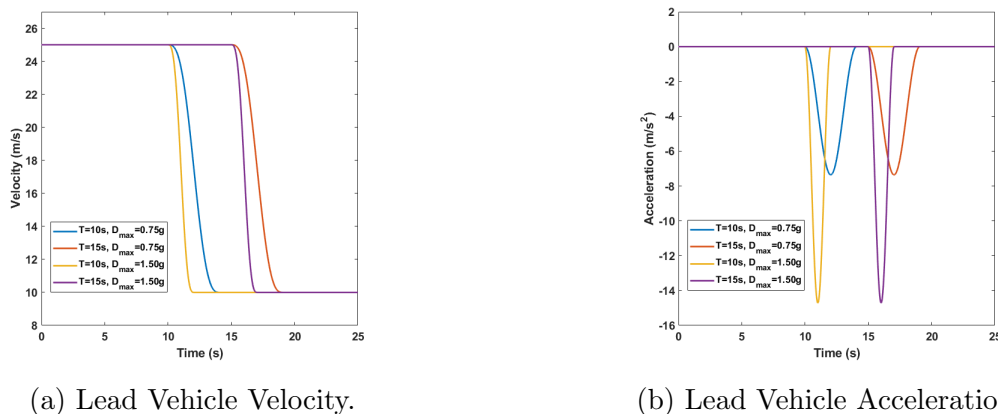
Figure 3.2: Stroop Effect Example. Note the incongruence between the color and text of the words.

### Lead Vehicle Braking Profile

In addition to the cognitive task given, the lead vehicle behavior was varied and presented in random order to avoid the subject anticipating the braking behavior. The following parameters were changed, resulting in 4 braking profiles:

- **Brake Application Time:** The lead vehicle started braking at  $t = 10$  seconds or 15 seconds, in each 25-second driving scenario.

<sup>3</sup><http://www.mathworks.com/matlabcentral/fileexchange/46596-stroop-test>



(a) Lead Vehicle Velocity.

(b) Lead Vehicle Acceleration.

Figure 3.3: Lead Vehicle Velocity and Acceleration for Braking Profiles Tested. The brake start time and max deceleration rates are indicated for each profile.

- **Brake Max Deceleration:** The lead vehicle used a smooth deceleration profile in PreScan to slow from 25 m/s to 10 m/s. The max deceleration allowed was either 0.75g or 1.5g.

Figure 3.3 shows the velocity and acceleration of the lead vehicle for the different braking profiles tested.

## Measurements

### Affective State

To characterize the affective state, EEG measurements and facial expression analysis were studied.

The EEG measurements were collected using a Muse 2014 EEG headband. This headband includes two forehead sensors (FP1 and FP2), two ear sensors (T9 and T10), and three reference sensors. Using the research tools developed by Muse <sup>4</sup>, the EEG data was transmitted over Bluetooth to a remote laptop.

A MS Kinect v2 and FLIR A665sc camera were used to capture variations in facial expression and temperature. The Kinect's depth and infrared streams were synchronized and calibrated with the thermal stream from the FLIR camera. Details on how these images were processed to capture thermal variations will be discussed in Section 3.4.

Further details on sensor setup (including camera calibration) can be found at [http://people.eecs.berkeley.edu/~govvijay/ms\\_supplement.html](http://people.eecs.berkeley.edu/~govvijay/ms_supplement.html).

<sup>4</sup><http://developer.choosemuse.com/research-tools>

### Perceived Workload

The NASA Task Load Index (TLX) survey was used to gauge how difficult subjects found each task. Figure 3.4 shows that subjects found the 2-back task to be the most challenging. On the other hand, the workload under 0-back was similar to having no secondary task.

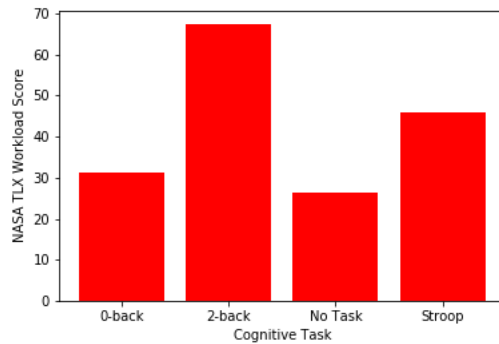


Figure 3.4: Average NASA TLX Workload Scores. Subjects found the workload under no task and 0-back conditions to be low, compared to the Stroop and 2-back tests. The 2-back test was considered the most challenging task to complete.

### Response

The response variable in this study was the brake reaction time of the subject,  $T_{RT}$ :

$$T_{RT} = t_{brake} - t^* \quad (3.1)$$

where  $t^*$  is when the lead car starts to decelerate (10s or 15s) and where  $t_{brake}$  is the first time the brake pedal is applied by the subject following  $t^*$ .

The reaction time, as well as relative kinematics, was determined using state information of the lead and ego vehicles collected using the PreScan software running the driving scenario simulations.

## 3.4 Methodology

In this section, we provide details on how features are generated from the affective sensing data and the relative kinematics between the lead and ego vehicles. We then give an overview of the algorithms investigated to do classification of the cognitive state and regression onto reaction time using these features.

### Feature Generation

There were three categories of features generated from the driving data and the affective sensing data: kinematic data, EEG data, and thermal facial data.

The relative kinematics between the lead and ego vehicle were determined using data collected with the PreScan software. The relative distance  $d_{rel}(t^*)$ , velocity  $v_{rel}(t^*)$ , and acceleration  $a_{rel}(t^*)$  at the lead vehicle’s brake start time  $t^*$  were used as kinematic features,  $\mathbf{x}_{kin}$ .

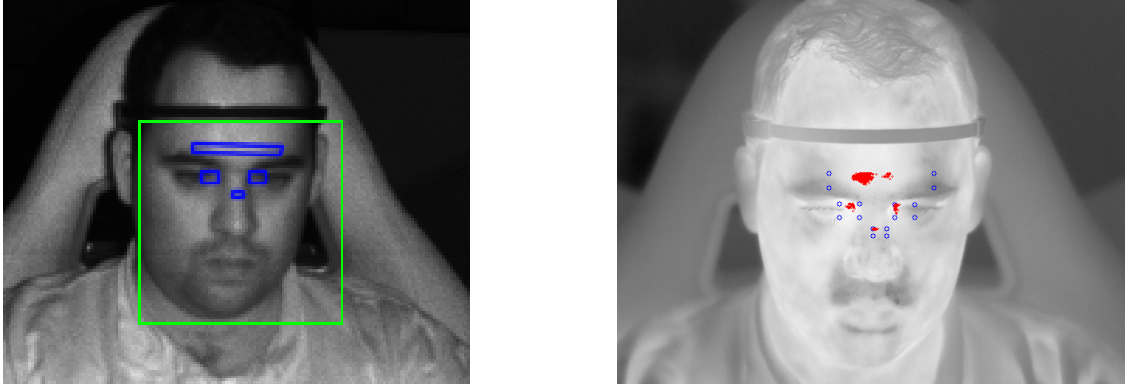
The second category of features,  $\mathbf{x}_{EEG}$ , came from the EEG data collected by the Muse. The mean and standard deviation by channel for each of the band power ranges in the list below was determined, using the 5-second window preceding the lead vehicle’s brake start time,  $t^*$ . These statistics were computed for both absolute intensity levels (Bels) and relative levels (normalized by the total signal power).<sup>5</sup> In addition, the Singular Spectrum Analysis (SSA) algorithm was applied to do a time-embedding of the 5-second time-series of relative band power data (averaged over the four channels to produce one time-series) preceding  $t^*$ . Principal Component Analysis (PCA) was then applied to reduce the SSA features to a 2-dimensional representation, using the code and approach developed by Ben Fulcher [12].

- delta (1-4 Hz)
- theta (4-8 Hz)
- alpha (7.5-13 Hz)
- beta (13-30 Hz)
- gamma (30-40 Hz)

The third category of features,  $\mathbf{x}_{thermal}$ , came from thermal facial analysis. Four regions of interest (ROIs) was selected based on prior thermal face imaging studies [41, 35]. These ROIs include the forehead, left eye, right eye, and nose. The Dlib face detector [23] was used to identify 68 facial points in the IR Kinect image. The IR points were projected to the thermal domain, using a pinhole camera model and camera calibration parameters found prior to experiments. Finally, the ROIs were identified in the thermal image. For each ROI, the mean of the top 10% of temperatures was recorded, to avoid capturing cooler elements like hair or the EEG headband. Figure 3.5 shows an example of this process.

<sup>5</sup><http://developer.choosemuse.com/research-tools/available-data>





(a) Face (green) and ROI detection (blue) in IR image using Dlib. (b) ROI detection in thermal image. Blue points represent the corners of each ROI. The red pixels indicate the location of top 10% temperatures within each ROI. The mean of these red points were used as thermal features.

Figure 3.5: Detection of Facial ROIs in IR domain and Projection to Thermal domain.

## Algorithm Details

There were three general problems we sought to solve with the aforementioned features ( $\mathbf{x}_{\text{kin}}$ ,  $\mathbf{x}_{\text{EEG}}$ , and  $\mathbf{x}_{\text{thermal}}$ ), as well as the cognitive task label ( $\mathbf{x}_{\text{cond}} \in \{1, 2, 3, 4\}$ , corresponding to No task, 0-back, 2-back, and Stroop task, respectively).

The first was to predict the reaction time ( $\hat{\mathbf{y}}_{\text{RT}}$ ) using:

1. Kinematics Alone:  $\mathbf{x} = \mathbf{x}_{\text{kin}}$
2. Kinematics and Cognitive Task Label:  $\mathbf{x} = [\mathbf{x}_{\text{kin}}, \mathbf{x}_{\text{cond}}]$
3. Kinematics and Affective Sensing:  $\mathbf{x} = [\mathbf{x}_{\text{kin}}, \mathbf{x}_{\text{EEG}}, \mathbf{x}_{\text{thermal}}]$

The second was to see if the cognitive task label could be predicted with the affective sensing data, i.e. use  $\mathbf{x}_{\text{thermal}}$  and  $\mathbf{x}_{\text{EEG}}$  to predict  $\mathbf{x}_{\text{cond}}$ .

The last problem was identical to the first problem, except that the predictions would be done using an online learning approach. Rather than simply getting the full training dataset of examples up front, the algorithm would get instances incrementally and update the model fit over time.

To solve the first and second tasks, we used K Nearest Neighbors and Random Forest algorithms. This was motivated by the observation of clustering and noise in the data that would be challenging to fit with parametric learning models. An example of the noisy data for one of the subjects is given in Figure 3.6.

To solve the third task, the K Nearest Neighbors algorithm was used but training data was provided incrementally. This algorithm is an online, instance-based learning approach.

For regression tasks, the mean squared error loss function was used to capture model fit. For the classification tasks, the label accuracy was computed. Scikit-Learn <sup>6</sup> was used to implement all the learning algorithms for the three problems of interest.

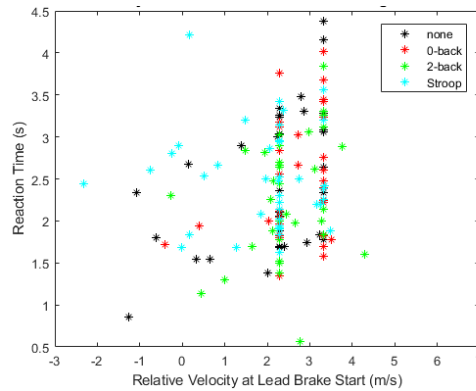


Figure 3.6: Noisy reaction time data for one of the subjects. Note the clustering and high variation in reaction time, even for a fixed relative velocity at  $t^*$ .

---

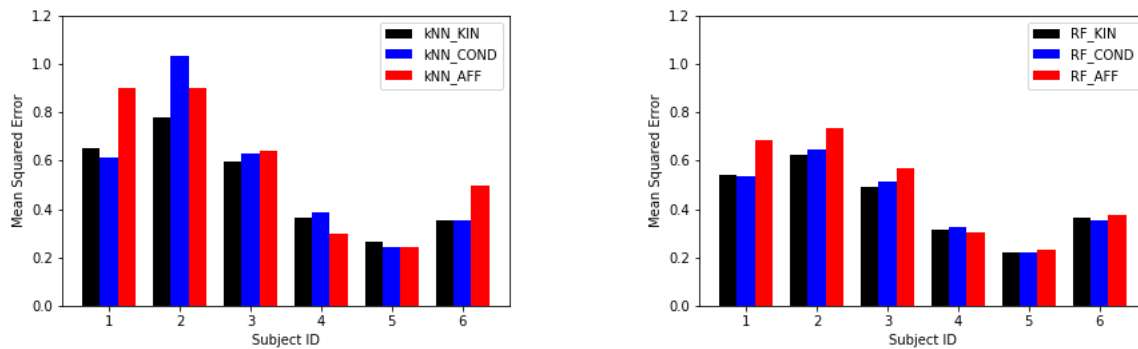
<sup>6</sup><http://scikit-learn.org/>

## 3.5 Results

In this section, we show the results of tackling the three problems mentioned in Section 3.4: offline regression of reaction time, offline classification of cognitive task, and online regression of reaction time.

### Offline Regression

Figure 3.7 shows the reaction time prediction error using kNN and RF algorithms. The reaction time prediction errors are generated using 4-fold cross validation and taking the average result. For the kNN algorithm, the number of neighbors ( $k$ ) was varied from 1 to 10, and the best result was kept. Similarly, for the RF algorithm, the max tree depth for a set of 20 trees was varied from 1 to 10, and the best result was kept. The RF algorithm slightly outperforms the kNN algorithm - reasonable given that RF uses an ensemble approach to lower variance. The key takeaway is that the affective state data does help to reduce model error for some of the subjects, although in general the affective state fit is slightly worse.



(a) Regression Results using kNN algorithm.

(b) Regression Results using RF algorithm.

Figure 3.7: Offline Regression Results for kNN and RF algorithms. For each subject, the model error is computed using kinematic features alone (black), kinematic features with the cognitive task label (blue), and kinematic features with affective data (red).

### Offline Classification

Figure 3.8 shows the results of trying to classify the cognitive task label using the affective state data only. As with the offline regression, the errors represent the best performance under 4-fold cross validation sweeping  $k$  from 1 to 10 and sweeping the depth of each tree in the forest from 1 to 10. The RF algorithm outperforms the kNN algorithm here, although classification accuracy is still quite low.

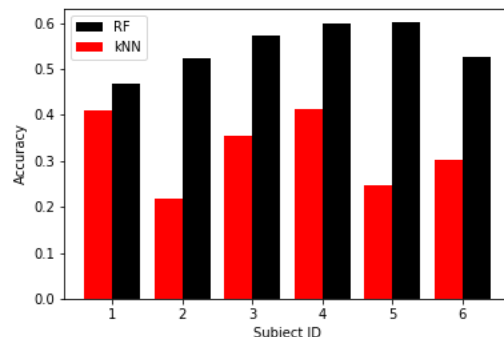


Figure 3.8: Classification Results using kNN and RF algorithms. The models were trained to predict the cognitive task label using affective state data only.

## Online Regression

In practice, the data will be collected incrementally, so the online regression algorithm was used to mimic that learning process. Figure 3.9 shows the learning curves on the data set as examples are presented incrementally to the kNN algorithm.

In the offline regression case, the assumption was the 75% of the data was used to generate the model (train set), and the model error was computed on the remaining 25% of the data (test set). This was done 4 times (4-fold cross validation), and the average was used to provide a model error estimate.

Here, we look at the regression problem from a different angle. Rather than splitting the data into train and test sets and fitting the data on the train set, as was done in the offline case, we assume there is only a train set. Examples from the train set are given sequentially to the online regression algorithm, which adapts its fit as each new data point is given. At each new example added, we compute the error on the full training set, given the subset of examples in the training set presented up to that point. Hence, when all the examples in the training set are given, the error goes to zero. Thus the focus here is not on the model error itself, but rather the learning curves showing how fast the online algorithm is learning to fit the training set.

Interestingly, for some subjects, the learning curve is quicker (i.e. lower error at a given number of instances) using the affective state information. This shows that there may be potential of using the affective state information to speed up online learning of the human model.

## 3.6 Discussion

In this chapter, we looked at the problem of combining online learning methods with affective sensing to develop personalized driver assistance systems. We focused on varying the cognitive workload through a set of secondary tasks and used EEG and thermal facial

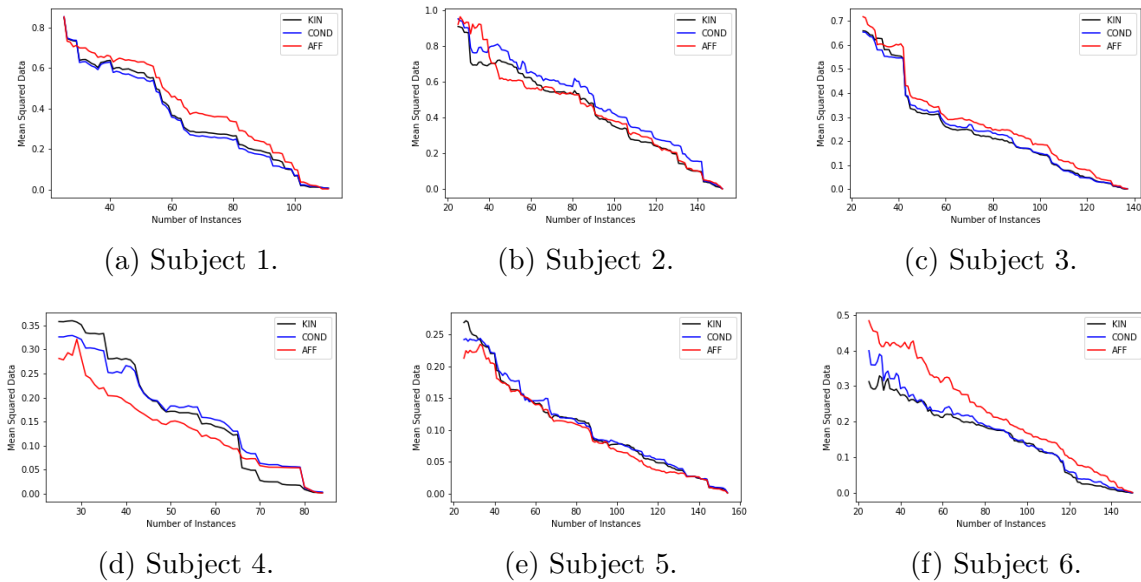


Figure 3.9: Online Regression Results for kNN algorithm with incremental addition of instances. Each plot corresponds to a different subject and shows the learning curve, i.e. how error on predicting the train set reaction times decreases as more examples from that set are added to the algorithm. For each subject, the learning curve is computed using kinematic features alone (black), kinematic features with the cognitive task label (blue), and kinematic features with affective data (red).

analysis to capture the driver’s affective state. We then developed algorithms to predict the driver’s brake reaction time under the different levels of cognitive workload, including an online version that improves as more instances or examples are given over time.

The results indicate the following:

1. Affective state information can help in some cases to reduce reaction time prediction error.
2. Trying to classify the cognitive task label is challenging but may not be needed to predict reaction time.
3. Affective state information can potentially speed up the reaction time prediction learning curve.

There are some limitations of the current approach. If these are addressed, the affective state information may prove even more useful:

1. **Curse of Dimensionality:** As more features are added, the density of examples reduces in the higher dimension space. This may be one of the key factors for why the high-dimensional affective state information is tough to use with a naive kNN approach

(i.e. using a Euclidean distance metric with uniform weights). Changing the distance metric to weight the most useful features would help to improve finding more similar neighbors, as in [36].

2. **Use of Cleaned EEG Signal:** The SSA algorithm was applied to the band power EEG data, but perhaps the raw EEG signal can be used after artifact removal to see if more informative EEG features can be generated.
3. **Addition of a Heuristic:** The kNN algorithm used didn't include a heuristic function: the approach was simply to wait until 25 examples were collected, then try to predict subsequent examples. Choosing an appropriate heuristic reaction time estimate might help with reducing error at the start of the learning process.

In addition, the low accuracy of the cognitive task label prediction may be due to limitations in the experimental design. Perhaps the driving scenario can be altered, so that examples are only collected in the middle of a long driving session under a specified cognitive task. With the current approach, a set of shorter, repeated driving scenarios were run, but the resets in between each scenario might have given a cognitive break to each subject and reduced the full impact of the cognitive secondary tasks.

Despite this fact, the affective state information still proved to be useful for predicting reaction time: suggesting that mapping the sensor values to a discrete label and then predicting reaction time may not be the right approach. Instead, the sensor data can be used directly to predict reaction time and avoid loss of information.

In terms of future work, there are several avenues that can be explored. The current approach involved post-processing the data, but a fully online experiment could be run where examples are stored as they are generated and the kNN algorithm updates in real-time. In addition, a driver study can be run to evaluate the impact of the reaction time estimate on the alert timing and whether it actually improves trust and acceptance of the alert system. A key aspect of that system would be to allow for both positive and negative feedback (i.e. the user can indicate whether the intervention was correct or not) and tune the stored examples accordingly for better behavior in subsequent interventions. Finally, this study involved measuring the affective state ahead of the intervention to predict the correct response. However, measuring the impact on affective state after the intervention would be an interesting way to characterize whether the intervention was good or bad, without requiring direct human feedback.

# Bibliography

- [1] Pieter Abbeel and Andrew Y. Ng. “Apprenticeship Learning via Inverse Reinforcement Learning”. In: *In Proceedings of ICML (2004)*.
- [2] Anayo K Akametalu et al. “Reachability-based safe learning with Gaussian processes”. In: *IEEE 53rd Annual Conference on Decision and Control (CDC)*. 2014, pp. 1424–1431.
- [3] M. Althoff, O. Stursberg, and M. Buss. “Stochastic Reachable Sets of Interacting Traffic Participants”. In: *IEEE Intelligent Vehicles Symposium*. June 2008, pp. 1086–1092. DOI: 10.1109/IVS.2008.4621131.
- [4] Narges Armanfard et al. “Vigilance lapse identification using sparse EEG electrode arrays”. In: *Electrical and Computer Engineering (CCECE), 2016 IEEE Canadian Conference on*. IEEE. 2016, pp. 1–4.
- [5] Vadim A Butakov and Petros Ioannou. “Personalized driver/vehicle lane change models for ADAS”. In: *IEEE Transactions on Vehicular Technology* 64.10 (2015), pp. 4422–4431.
- [6] Suhas E Chelian et al. “Reinforcement learning and instance-based learning approaches to modeling human decision making in a prognostic foraging task”. In: *Development and Learning and Epigenetic Robotics (ICDL-EpiRob), 2015 Joint IEEE International Conference on*. IEEE. 2015, pp. 116–122.
- [7] E Coelingh et al. *Collision Warning With Auto Brake - A Real-Life Safety Perspective*. Apr. 2007.
- [8] Erez Dagan et al. “Forward collision warning with a single camera”. In: *Intelligent Vehicles Symposium, 2004 IEEE*. IEEE. 2004, pp. 37–42.
- [9] K. Driggs-Campbell and R. Bajcsy. “Identifying Modes of Intent from Driver Behaviors in Dynamic Environments”. In: *IEEE 18th International Conference on Intelligent Transportation Systems (ITSC)*. Sept. 2015, pp. 739–744. DOI: 10.1109/ITSC.2015.125.
- [10] Katherine Driggs-Campbell, Vijay Govindarajan, and Ruzena Bajcsy. “Integrating Intuitive Driver Models in Autonomous Planning for Interactive Maneuvers”. In: *IEEE Transactions on Intelligent Transportation Systems (2017)*. DOI: 10.1109/TITS.2017.2715836.



- [11] Katherine Driggs-Campbell, Victor Shia, and Ruzena Bajcsy. “Improved Driver Modeling for Human-in-the-Loop Control”. In: *2015 IEEE International Conference on Robotics and Automation*. May 2015.
- [12] Ben D Fulcher and Nick S Jones. “hctsa: A Computational Framework for Automated Time-Series Phenotyping Using Massive Feature Extraction”. In: *Cell systems* 5.5 (2017), pp. 527–531.
- [13] Jeremy H Gillula and Claire J Tomlin. “Reducing Conservativeness in Safety Guarantees by Learning Disturbances Online: Iterated Guaranteed Safe Online Learning”. In: *Robotics: Science and Systems* (2013), p. 81.
- [14] Cleotilde Gonzalez, Javier F Lerch, and Christian Lebiere. “Instance-based learning in dynamic decision making”. In: *Cognitive Science* 27.4 (2003), pp. 591–635.
- [15] Larry Greenemeier. “When Your Self-Driving Car Wants to Be Your Friend, Too”. In: *Scientific American* (Jan. 12, 2017). URL: <https://www.scientificamerican.com/article/when-your-self-driving-car-wants-to-be-your-friend-too/>.
- [16] John Halkias and James Colyar. “Next Generation SIMulation Fact Sheet”. In: *US Department of Transportation: Federal Highway Administration*. Dec. 2006.
- [17] Sandra G Hart. “NASA-task load index (NASA-TLX); 20 years later”. In: *Proceedings of the human factors and ergonomics society annual meeting*. Vol. 50. 9. Sage Publications Sage CA: Los Angeles, CA. 2006, pp. 904–908.
- [18] David Henriques et al. “Statistical Model Checking for Markov Decision Processes”. In: *9th IEEE International Conference on Quantitative Evaluation of Systems (QEST)*. 2012, pp. 84–93.
- [19] Adam Houenou et al. “Vehicle Trajectory Prediction based on Motion Model and Maneuver Recognition”. In: *IEEE/RSJ International Conference on Intelligent Robots and Systems (IROS)*. IEEE, 2013, pp. 4363–4369.
- [20] Stephanos Ioannou, Vittorio Gallese, and Arcangelo Merla. “Thermal infrared imaging in psychophysiology: potentialities and limits”. In: *Psychophysiology* 51.10 (2014), pp. 951–963.
- [21] A Hamish Jamson, Frank CH Lai, and Oliver MJ Carsten. “Potential benefits of an adaptive forward collision warning system”. In: *Transportation research part C: emerging technologies* 16.4 (2008), pp. 471–484.
- [22] Nikolaos Kariotoglou et al. “Multi-Agent Autonomous Surveillance: A Framework Based on Stochastic Reachability and Hierarchical Task Allocation”. In: *Journal of Dynamic Systems, Measurement, and Control* 137.3 (2015), p. 031008.
- [23] Davis E King. “Dlib-ml: A machine learning toolkit”. In: *Journal of Machine Learning Research* 10.Jul (2009), pp. 1755–1758.

- [24] Stéphanie Lefèvre, Ashwin Carvalho, and Francesco Borrelli. “A learning-based framework for velocity control in autonomous driving”. In: *IEEE Transactions on Automation Science and Engineering* 13.1 (2016), pp. 32–42.
- [25] Chin-Teng Lin et al. “EEG-based drowsiness estimation for safety driving using independent component analysis”. In: *IEEE Transactions on Circuits and Systems I: Regular Papers* 52.12 (2005), pp. 2726–2738.
- [26] Christine L Lisetti and Fatma Nasoz. “Affective intelligent car interfaces with emotion recognition”. In: *Proceedings of 11th International Conference on Human Computer Interaction, Las Vegas, NV, USA*. 2005.
- [27] Nick Malone et al. “Stochastic Reachability Based Motion Planning for Multiple Moving Obstacle Avoidance”. In: *Proceedings of the 17th International Conference on Hybrid Systems: Computation and Control*. ACM. 2014, pp. 51–60.
- [28] Bruce Mehler et al. “Impact of incremental increases in cognitive workload on physiological arousal and performance in young adult drivers”. In: *Transportation Research Record: Journal of the Transportation Research Board* 2138 (2009), pp. 6–12.
- [29] Ian M. Mitchell. “Comparing Forward and Backward Reachability as Tools for Safety Analysis”. In: *10th International Workshop on Hybrid Systems: Computation and Control (HSCC)*. 2007, pp. 428–443. ISBN: 978-3-540-71493-4. DOI: 10.1007/978-3-540-71493-4\_34.
- [30] Ian M Mitchell, Alexandre M Bayen, and Claire J Tomlin. “A Time-Dependent Hamilton-Jacobi Formulation of Reachable Sets for Continuous Dynamic Games”. In: *IEEE Transactions on Automatic Control* 50.7 (2005), pp. 947–957.
- [31] Ian M. Mitchell and Jeremy A. Templeton. “A Toolbox of Hamilton-Jacobi Solvers for Analysis of Nondeterministic Continuous and Hybrid Systems”. In: *8th International Workshop on Hybrid Systems: Computation and Control (HSCC)*. 2005, pp. 480–494. ISBN: 978-3-540-31954-2. DOI: 10.1007/978-3-540-31954-2\_31.
- [32] Andrew F. Monk et al. “N-backer: An auditory n-back task with automatic scoring of spoken responses”. In: *Behavior Research Methods* 43.3 (Mar. 2011), p. 888. ISSN: 1554-3528. DOI: 10.3758/s13428-011-0074-z. URL: <https://doi.org/10.3758/s13428-011-0074-z>.
- [33] Mariella Moon. “Jaguar adapts NASA tech to monitor brainwaves and avoid accidents”. In: *Engadget* (June 19, 2015). URL: <https://www.engadget.com/2015/06/19/jaguar-sixth-sense-safety-tech/>.
- [34] New York State Department of Motor Vehicles. “NYS DMV - Driver’s Manual - Chapter 8: Defensive Driving”. In: (Sept. 2001).
- [35] BR Nhan and Tom Chau. “Infrared thermal imaging as a physiological access pathway: a study of the baseline characteristics of facial skin temperatures”. In: *Physiological measurement* 30.4 (2009), N23.

- [36] Roberto Paredes and Enrique Vidal. “Learning weighted metrics to minimize nearest-neighbor classification error”. In: *IEEE Transactions on Pattern Analysis and Machine Intelligence* 28.7 (2006), pp. 1100–1110.
- [37] Hae Won Park and Ayanna M Howard. “Retrieving experience: Interactive instance-based learning methods for building robot companions”. In: *Robotics and Automation (ICRA), 2015 IEEE International Conference on*. IEEE. 2015, pp. 6140–6145.
- [38] Ioannis Pavlidis et al. “Interacting with human physiology”. In: *Computer Vision and Image Understanding* 108.1 (2007), pp. 150–170.
- [39] Stephen Prajna, Ali Jadbabaie, and George J Pappas. “A Framework for Worst-Case and Stochastic Safety Verification Using Barrier Certificates”. In: *IEEE Transactions on Automatic Control* 52.8 (2007), pp. 1415–1428.
- [40] Colin Puri et al. “StressCam: non-contact measurement of users’ emotional states through thermal imaging”. In: *CHI’05 extended abstracts on Human factors in computing systems*. ACM. 2005, pp. 1725–1728.
- [41] Colin Puri et al. “StressCam: non-contact measurement of users’ emotional states through thermal imaging”. In: *CHI’05 extended abstracts on Human factors in computing systems*. ACM. 2005, pp. 1725–1728.
- [42] Dawn M. Schiehser and Mark W. Bondi. “Stroop Color-Word Test”. In: *The Corsini Encyclopedia of Psychology*. John Wiley and Sons, Inc., 2010. ISBN: 9780470479216. DOI: 10.1002/9780470479216.corpsy0951. URL: <http://dx.doi.org/10.1002/9780470479216.corpsy0951>.
- [43] V.A Shia et al. “Semiautonomous Vehicular Control Using Driver Modeling”. In: *IEEE Transactions on Intelligent Transportation Systems* PP.99 (2014), pp. 1–14. ISSN: 1524-9050. DOI: 10.1109/TITS.2014.2325776.
- [44] Elisabeth A Strunk, M Anthony Aiello, and John C Knight. “A Survey of Tools for Model Checking and Model-Based Development”. In: *University of Virginia* (2006).
- [45] P. Varaiya. “Smart cars on smart roads: problems of control”. In: *IEEE Transactions on Automatic Control* 38.2 (1993), pp. 195–207. ISSN: 0018-9286. DOI: 10.1109/9.250509.
- [46] R. Vasudevan et al. “Safe semi-autonomous control with enhanced driver modeling”. In: *American Control Conference*. 2012, pp. 2896–2903.
- [47] Kemin Zhou and John Comstock Doyle. *Essentials of Robust Control*. Vol. 104. Prentice Hall, Upper Saddle River, NJ, 1998.